

DESIGN AND TESTING OF SEED PUSH WHEEL FOR HIGH-SPEED PRECISION SEED METERING DEVICE FOR CORN WITH INTERNAL SEED FILLING AND POSITIVE PRESSURE AIRFLOW

玉米内充气压式高速精量排种器推种轮设计与试验

Xin DU, Qianhao YU, Shufa CHEN, Qixin SUN, Han ZHANG, Changqing LIU*

School of Mechanical Engineering, Jiangsu Ocean University, Lianyungang 222005/ China

Tel: 0086-0518-85895322; E-mail: lyg_lcq@163.com

Corresponding author: Changqing Liu

DOI: <https://doi.org/10.35633/inmateh-72-65>

Keywords: Precision seeding device; Seed push wheel; High-speed; Precision agriculture

ABSTRACT

In order to improve the uniformity and stability of seed delivery and meet the requirements of precision sowing operation, a kind of seed push wheel designed to mesh with the seed discharging disk was developed. The wheel underwent theoretical analysis and experimental optimization regarding parameters such as tooth profile, tooth count, and tooth height. Using a pneumatically inflated maize precision seed-metering device as the seeding carrier, a full-factorial experiment was conducted with operational speed and tooth height as the experimental variables, and qualification rate, reseeding rate, and leakage rate as the performance indicators. A multivariate quadratic regression model was established to assess the relationships between the factors and indicators. The results indicated that optimal seed guiding performance was achieved when the seed push wheel had 9 teeth, a tooth height of 5.2–6.2 mm, and an operational speed of 9.0–12.6 km/h. This study provides a theoretical foundation and data support for the development of precision seeding technology and corresponding seed guiding devices.

摘要

为提高导种投送均匀性与稳定性, 满足精量播种作业要求, 设计了一种与排种盘啮合传动的推种轮, 对其齿形参数、齿数、凸齿高度等因素进行了理论分析与试验优化。以气压内充式玉米精量排种器为排种载体, 结合全因素试验, 以作业速度和凸齿高度为试验因素, 合格率、重播率和漏播率为试验指标, 建立了因素与指标间的多元二次回归模型。结果表明, 当推种轮齿数为9、推种轮凸齿高度为5.2–6.2 mm、作业速度为9.0–12.6 km/h时, 导种性能最佳。本研究可为精量播种技术及配套导种装置的研制提供理论基础与数据支撑。

INTRODUCTION

Corn is an important feed, energy and industrial crop, and its cultivation area and output have ranked first in China for many years (Yang *et al.*, 2016). China's per capita arable land area is less than half of the world's per capita level, in the context of sustained population growth and arable land area remains unchanged or even decreased, to ensure the efficient production of maize, that is, to improve yields is the key to solving the problem of food security (Tang *et al.*, 2019; Yuan *et al.*, 2018). Factors affecting corn yields are climate, soil conditions, seeds, planting techniques and field management techniques, among which seeding quality is one of the most important influencing factors. In order to improve the seeding quality of mechanized operations, over the years, the precision seed discharger (Karayel *et al.*, 2022; Kumar-Patel *et al.*, 2021; Ospanova *et al.*, 2024) has been the focus of research and hot spots of single grain (precision) seeding machine, while for high-speed operations (>9 km/h) the research of smooth seeding mechanism is relatively weak, the seed guide, seeding link has become a constraint on the quality of high-speed sowing operations to further improve the "short board", there is an urgent need to develop the high-speed operation of the smooth seeding mechanism (Liao *et al.*, 2020).

Xin Du, Lecturer Ph.D. Eng; Qianhao Yu, MA.Eng Stud.; Shufa Chen, Prof. Ph.D. Eng; Qixin Sun, Prof. Ph.D. Eng; Han Zhang, B.S Stud.; Changqing Liu*, Lecturer Ph.D. Eng.

Currently, improving corn seed spacing uniformity typically involves lowering the height of seed casting. However, at high speeds, the moment the seed enters the seed bed cannot fully compensate for the relative speed difference of the machine, resulting in a significant decrease in grain spacing uniformity (Fanigliulo *et al.*, 2022). Additionally, the absence of synchronized contour wheels for sowing monomers with automatic depth control leads to inconsistencies in sowing depth. After the addition of synchronous contour wheels to the seeding unit, the increased seeding height necessitates the use of corrugated tubes to guide the seeds accurately into the planting furrow. However, the random movement of seeds within the tube can lead to collisions and bouncing, resulting in reduced uniformity in seed spacing (Awad *et al.*, 2022; Im *et al.*, 2023).

Liu *et al.* (2015) used three-dimensional reverse engineering to improve the curved seed guide tube, based on the "zero-speed seeding" method, which reduces the horizontal bouncing and slipping of the seeds. Zhao *et al.* (2018) designed a V-shaped groove paddle wheel-type seed guide component, which can actively adjust the state of seed movement after seed discharging. Qi *et al.* (2015) designed a centralized exhaust-fed corn precision seed discharger, which adopts positive pressure airflow to convey and guide seeds. Li *et al.* (2020) analysed and established the relationship and mathematical model between the length of the air-fed seed guide tube and the airflow velocity inside the tube. Chen *et al.* (2012) designed a belt-type seed guide device integrated with the transmission and seed casting mechanism, which made the seeds move to the seed casting position according to a predetermined trajectory and improved the coefficient of variation of the grain spacing. Liu *et al.* (2017) proposed a seeding technology of precise seed picking, smooth seed delivery and precise seed casting, and designed a seeding synchronous belt-type seed guide device.

The above scholars have researched various types of seed-guiding components from the aspects of component structure, parameter optimization and influencing factors, and have also made certain research progress, but they have not completely restricted the seed degrees of freedom during the seed-guiding process, and cannot avoid the collision bouncing of the seeds in the seed-guiding tubes, and the uniformity of the grain spacing during the high-speed operation is poor. In this context, in order to improve the uniformity and stability of seed guide delivery, design a kind of seed push wheel with the matching transmission of seed discharge disk, analyse the influence of each parameter on the performance of the seed guide, and validate the reasonableness of the design through the bench test, with a view to providing theoretical references and data support for the research and development of the supporting seed guide device.

MATERIALS AND METHODS

Structure and key parameters

This group designed a high-speed smooth seed delivery mechanism for corn based on full-degree-of-freedom constrained seed guiding, which is used in conjunction with the high-speed precision seed discharger for corn developed in the previous stage, the working principle and structural composition of which have been clearly described in the published literature (Du and Liu, 2023), and the working process can be divided into three tandem links of pushing, guiding, and casting the seed (as shown in Fig. 1).

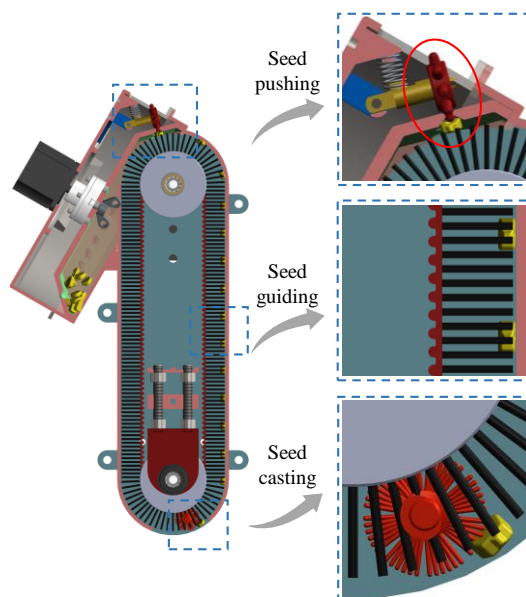


Fig. 1 – Schematic diagram of the full-degree-of-freedom constrained seed-guiding process

In order to make the seeds accurately embedded in the bristles on the brush belt, a seed push wheel setup suitable for high-speed seeding is designed by utilizing the principle of gear meshing, as shown in Fig.2. The seed push wheel consists of seed push wheel fixing device, pressure spring, seed push wheel, seed push wheel axle and bearing, etc., in which the convex teeth on the seed push wheel mesh with the type holes and concave teeth on the seed discharging disk. When working, the seed discharge disk is driven by a stepping motor to rotate, and the seed discharge disk rotates to drive the seed push wheel to follow. When the convex teeth on the seed push wheel enter the holes on the seed plate, they block airflow escape, reducing pressure on the surface of the seeds. Additionally, the increased depth of convex teeth penetration into the holes helps dislodge seeds attached to the hole surface, embedding them into the bristles of the brush.

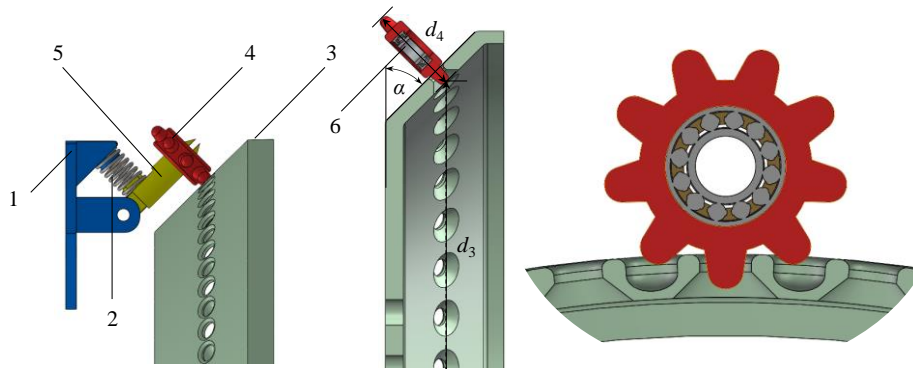


Fig. 2 – Schematic diagram of seed push wheel structure

1. seed wheel retainer 2. compression spring 3. seed discharge disk 4. seed wheel 5. seed wheel axle 6. bearing.
 α : cone angle; d_4 : diameter of tooth apex circle; d_3 : diameter of seed discharge disc at engagement

In order to make the convex teeth mesh smoothly with the concave teeth and holes, the movement between the seed pushers and seed disks should be regarded as pure rolling, and the distance between the holes on the seed disks should be equal to or a multiple of the distance between the teeth of the convex teeth of the seed pushers.

$$\frac{2\pi R}{Z} = K \frac{2\pi r}{z} \quad (1)$$

where: R is the circumferential radius of the hole in the seed discharge disk, mm; Z is the number of holes in the seed discharge disk; K is a constant, take 1 or 2; r is the radius of the base circle of the seed push wheel, mm; z is the number of teeth on the seed push wheel.

It is known that the circumferential radius R of the hole in the seed discharge disk is 99.5 mm, the number of holes Z on the seed discharge disk is 36, and the number of teeth z on the seed push wheel is 9. According to the above formula, the radius of the base circle of the seed push wheel can be obtained as 24.875 mm or 14.4375 mm, which corresponds to the K of 1 and 2, respectively. As the space available for installing the seed push device in the seed dispenser is not large, the radius of the base circle of the seed push wheel is taken to be 14.4375 mm, and at this time, K is 2, and a concave tooth is dug between every 2 holes to realize the normal meshing with the seed push wheel.

As the seed plate drives the seed push wheel's rotation, the convex teeth of the seed push wheel mesh with the concave teeth and holes on the seed plate. During this process, the engagement point on the seed plate remains constant at point B' , causing the convex teeth of the seed push wheel to slide and mesh along point B' . In order to calculate the tooth shape formula of the convex teeth, this paper adopts the "reverse method" to inverse the trajectory of B' .

As illustrated in Figure 3, assuming the seed push wheel remains stationary, the motion relationship between the seed plate and the seed push wheel remains unchanged according to the principle of relative motion. This implies that the seed plate undergoes pure rolling motion along the seed push wheel. At a certain moment, the seed plate is positioned at number 1, and the engagement point on the seed push wheel is point B , while the engagement point on the seed plate is point B' . After a period of time, when the seed plate rotates around the centre O of the seed push wheel by an angle θ and reaches position number 2, the engagement point on the seed push wheel is at point A . The trajectory of the engagement point on the seed plate, represented by B' , follows the tooth profile curve of the seed push wheel.

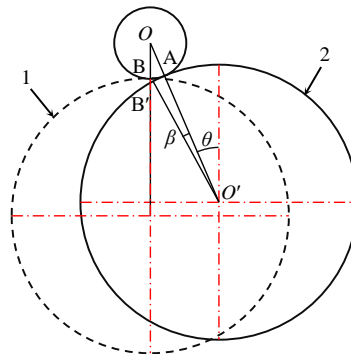


Fig. 3 – Design of convex tooth profile for seed pushers

1. initial position 2. position after relative rotation

O: seed push wheel centre; B and B' are the initial and "post-reversal" engagement points, respectively; O': seeding wheel centre; A: engagement point after rotation of the seed push wheel; θ : Angle of rotation of the seeding wheel around point O at the centre of the seed push wheel; β : angle of $\angle AO'B'$.

Establish a coordinate system with the centre O of the seed push wheel as the origin, so that $\angle AO'B'$ is β , then the coordinates of O' and B' are respectively:

$$O'[(R+r)\sin\theta, (R+r)\cos\theta] \tag{2}$$

$$B'[(R+r)\sin\theta - R\sin(\theta + \beta), (R+r)\cos\theta - R\cos(\theta + \beta)] \tag{3}$$

Since the form of motion between the seed discharge disk and the seed push wheel is pure rolling, according to the geometrical relationship there is:

$$\begin{cases} AB = AB' \\ \theta r = \beta R \end{cases} \tag{4}$$

i.e.

$$\beta = \frac{\theta r}{R} \tag{5}$$

From the above equation, the coordinates of B' can be expressed as:

$$B' \left[(R+r)\sin\theta - R\sin\left(\theta\left(1 + \frac{r}{R}\right)\right), (R+r)\cos\theta - R\cos\left(\theta\left(1 + \frac{r}{R}\right)\right) \right] \tag{6}$$

Thus the parametric equation of the displacement curve for point B' can be expressed as:

$$\begin{cases} x = (R+r)\sin\theta - R\sin\left(\theta\left(1 + \frac{r}{R}\right)\right) \\ y = (R+r)\cos\theta - R\cos\left(\theta\left(1 + \frac{r}{R}\right)\right) \end{cases} \tag{7}$$

According to the previously determined radius R of the seed discharge disk and the radius r of the base circle of the seed push wheel, the tooth shape formula of the convex teeth of the seed push wheel can be obtained as follows:

$$\begin{cases} x = 113.9375\sin\theta - 99.5\sin(1.1451\theta) \\ y = 113.9375\cos\theta - 99.5\cos(1.1451\theta) \end{cases} \tag{8}$$

Similarly, as shown in Figure 4, assuming that the push seed wheel remains stationary, assuming the seed push wheel remains stationary, the seed plate rotates counterclockwise relative to the seed push wheel.

At a certain moment, when the seed plate is positioned at number 1, the engagement point on the seed push wheel is point B, while the engagement point on the seed plate is point B'; after a period of time, when the seed discharge disc rotates around the centre of the seed push wheel O by an angle of θ and is located at the position of serial number 2, the engagement point of the seed push wheel becomes point A, and the movement trajectory of the engagement point on the seed discharge disc is B', which is the convex tooth profile of the seed push wheel.

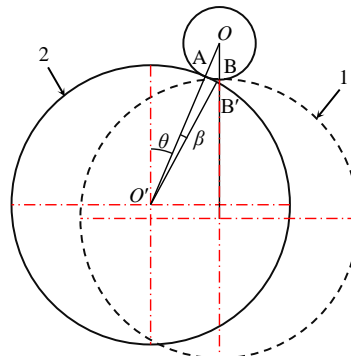


Fig. 4 – Schematic diagram of engagement and separation points

1. initial position 2. position after relative rotation

O: seed push wheel centre; B and B' are the initial and "post-reversal" engagement points, respectively; O': seeding wheel centre; A: engagement point after rotation of the seed push wheel; θ : Angle of rotation of the seeding wheel around point O at the centre of the seed push wheel; β : angle of $\angle AO'B'$.

Similar to the derivation of the tooth profile of the seeding wheel, a parametric equation for the displacement profile of the point B' can be obtained:

$$\begin{cases} x = -(R+r)\sin\theta + R\sin\left(\theta\left(1+\frac{r}{R}\right)\right) \\ y = (R+r)\cos\theta - R\cos\left(\theta\left(1+\frac{r}{R}\right)\right) \end{cases} \quad (9)$$

Comparing Eq. (7) and Eq. (9), it can be seen that the two curves are symmetric about the y-axis.

In order to ensure that the convex teeth on the seed push wheel and the concave teeth and holes on the seed discharging disk are normally engaged, it should be ensured that when the convex teeth are disengaged from the concave teeth or holes, the next pair of teeth just start to mesh, and at this time, the convex teeth on the seed push wheel are engaged with the concave teeth and holes on the seed discharging disk at the maximum depth, as shown in Fig. 5.

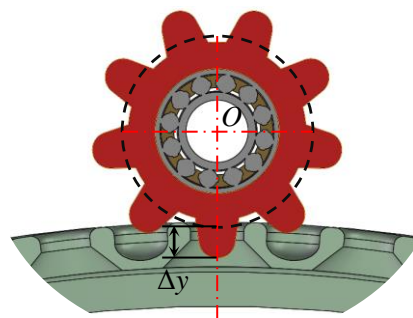


Fig. 5 – Engagement depth schematic

Δy : the maximum depth of engagement

The maximum depth of engagement Δy is the difference between the maximum value (extreme value) of the longitudinal coordinate equation of the tothing curve of the convex teeth of the seed pushers and its initial value. Since the longitudinal curve of the tooth shape of the convex teeth of the seed pushers is symmetric about the x-axis, the maximum depth of engagement Δy can be obtained by solving the parametric equation of any one of the curves, and the derivation of y .

$$y' = -113.9375\sin\theta + 99.5 \times 1.1415\sin(1.1451\theta) \quad (10)$$

Make $y' = 0$, then get $\theta = 0^\circ$ or 240.4081° , will be substituted into the formula (10), the maximum value of y is 14.4375 mm or 18.64 mm, so as to get the maximum depth of engagement Δy is 0 mm or 4.2 mm. Based on the above formulas, the convex tooth profile of the seed push wheel was obtained. To prevent mechanical damage to the seeds during the pushing process and to facilitate meshing and machining, the tooth tops of the convex teeth were rounded, resulting in the convex tooth profile shown in Figure 5.

Bench testing

In order to verify the accuracy of the theoretical analysis and the hole formation performance of the internal pneumatic precision seed discharger under different working parameters, the parts were injection moulded using the Dimension Elite 3D printer (precision 0.178 mm, material ABS) produced by Stratasys Company of the United States. The seed guiding performance was tested on the JPS-12 multifunctional seed discharging test, and a layer of 1~2 mm thick grease was applied on the conveyor belt of the test stand to prevent the corn seeds from bouncing, and the test setup is shown in Figure 6. The corn variety "Zhengdan 958", which has the largest planting area in China, was utilized as the test subject.

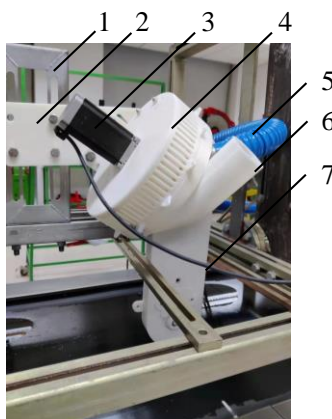


Fig. 6 – Schematic diagram of seed-guiding device bench test

1. seed dispenser fixing frame; 2. seed dispenser fixing plate; 3. seed dispenser drive motor;
4. pneumatic seed dispenser; 5. air inlet pipe; 6. seed inlet; 7. seed guide device

Test indicators

In order to evaluate the operational performance of the seed-guiding device, according to GB/T 6973-2005 Test Methods for Single Grain (Precision) Seeders, single grain rate, reseeding rate, leakage rate and grain spacing coefficient of variation are used as evaluation indexes. The formula for calculating each performance index is as follows

$$\begin{cases} Y_1 = \frac{n_s}{n_0} \times 100\% \\ Y_2 = \frac{n_d}{n_0} \times 100\% \\ Y_3 = \frac{n_m}{n_0} \times 100\% \end{cases} \quad (11)$$

Where: Y_1 is the qualified rate, %; Y_2 is the multiple rate, %; Y_3 is the leakage rate, %; n_s is the number of qualified seed holes, count; n_d is the number of double or more seed holes, count; n_m is the number of empty holes, count; and n_0 is the total number of holes of the test seeds, 251 holes.

Due to the length constraint of the conveyor belt, data were collected from 251 maize seed holes each time. Each treatment was repeated three times and average values were calculated. The data were organized to determine the qualified rate, multiple rate and leakage rate.

RESULTS

Number of teeth on the seed pushers

Different quantities of convex teeth on the seed push wheel result in varying linear speeds during operation. This variation alters the mechanical performance when the seed push wheel engages with the seed plate, thereby impacting the seed discharge qualification rate.

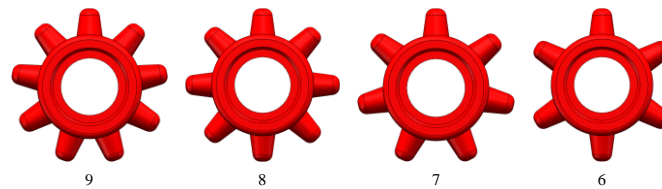


Fig. 7 – Schematic diagram of the number of teeth on the seed pushers

As shown in Fig. 7, seed pushers with different numbers of teeth were modelled in SolidWorks, and seed disks with different numbers of concave teeth were modelled considering that seed pushers were used in conjunction with seed disks. Under the conditions of operating speed of 10 km/h, air pressure of 1.6 kPa, respectively, a one-factor simulation test was carried out with the number of teeth of the seed pushers as the factor and the seed discharge pass rate as the target, and the test results were shown in Figure 8.

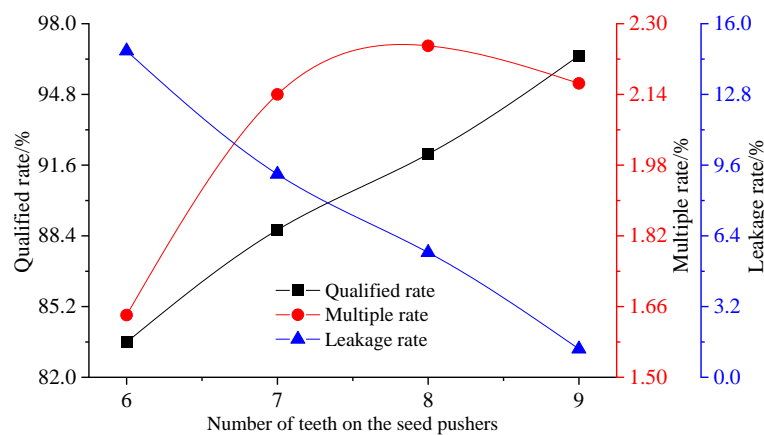


Fig. 8 – Schematic diagram of the number of teeth on the seed pushers

As shown in Figure 8, increasing the number of convex teeth on the seed push wheel leads to a linear decrease in the missing seed rate. This occurs because an increased number of convex teeth reduces the linear speed of the seed plate and ensures smoother meshing between the seed push wheel and the seed plate, minimizing vibrations in the seed plate. Consequently, the leakage rate decreases, while qualified and multiple rates improve.

Height of seed pushers' teeth

The height of the convex teeth of the seed push wheel directly affects the depth of the convex teeth into the concave teeth, which has an important impact on the timely introduction of seeds from the hole. On the premise of not affecting the normal meshing relationship between the seed push wheel and the seed discharge disk, the height of the convex teeth of the seed push wheel is set to 4.2 mm, 4.7 mm, 5.2 mm and 5.7 mm, respectively, and the height of the convex teeth of the seed push wheel is shown in Figure 9.

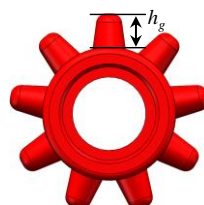


Fig. 9 – The height of the seed pushers' cams
 h_g : tooth height

Under the conditions of operating speed of 10 km/h, air pressure of 1.6 kPa, the number of teeth of the seed push wheel is 9, respectively, and the height of the convex teeth of the seed push wheel is taken as the factor to carry out a one-factor simulation test with the qualified rate of seed discharging as the target, and the test results are shown in Fig. 10.

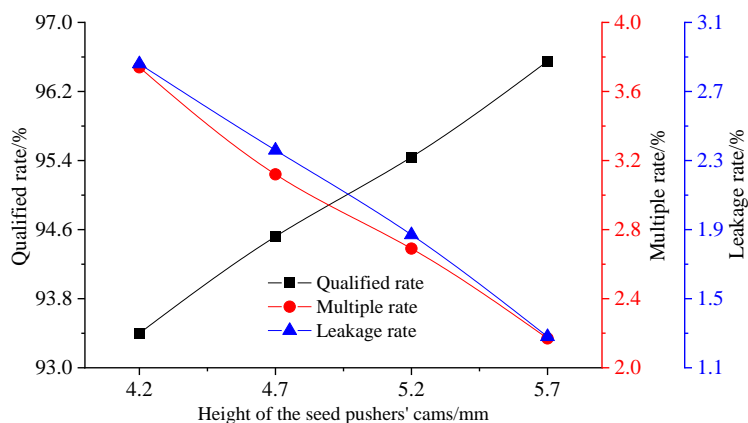


Fig. 10 – Influence of the height of the seed pushers' cams on the performance of seed discharging

As can be seen from Fig. 10, the qualified rate decreases linearly when the tooth height of the convex teeth of the seed push wheel decreases, because the seed cannot be pushed out of the surface of the moulded hole and embedded in the brush bristles in time after the tooth height decreases, resulting in an increase in the leakage rate and the re-seeding rate. Increasing the tooth height without affecting the normal engagement can push the seed away from the surface of the mould hole for a sufficiently large distance to embed the seed in the bristles.

Interactions among the factors

Based on the above analysis, the number of teeth on the seed pushers was determined to be 9. In order to study the effect of the interaction between the working speed and the height of the seed pushers' cams on the target results, a full factorial test was designed with the working speed and the height of the seed pushers' cams as the study factors, and the qualified rate, multiple rate and leakage rate were used as the study objectives.

The test scheme and test results are shown in Table 1.

Table 1

Full factorial test program and results					
No.	Speed v_m (km/h)	Height h_g (mm)	Qualified y_1 (%)	Multiple y_2 (%)	Leakage y_3 (%)
1	7.2	4.7	93.17	2.38	4.45
2	7.2	5.2	94.95	2.07	2.98
3	7.2	5.7	95.66	1.69	2.65
4	7.2	6.2	95.29	1.25	3.46
5	7.2	6.7	93.85	0.73	5.42
6	9.0	4.7	93.59	2.67	3.74
7	9.0	5.2	95.40	2.36	2.25
8	9.0	5.7	96.13	1.97	1.89
9	9.0	6.2	95.80	1.52	2.69
10	9.0	6.7	94.38	1.00	4.62
11	10.8	4.7	93.68	2.76	3.56
12	10.8	5.2	95.52	2.44	2.04
13	10.8	5.7	96.29	2.05	1.66
14	10.8	6.2	95.98	1.59	2.43
15	10.8	6.7	94.59	1.06	4.35
16	12.6	4.7	93.46	2.65	3.89
17	12.6	5.2	95.33	2.32	2.35
18	12.6	5.7	96.12	1.93	1.96
19	12.6	6.2	95.84	1.46	2.70
20	12.6	6.7	94.48	0.93	4.59
21	14.4	4.7	92.91	2.34	4.75
22	14.4	5.2	94.81	2.01	3.19
23	14.4	5.7	95.63	1.61	2.77
24	14.4	6.2	95.37	1.13	3.49
25	14.4	6.7	94.05	0.59	5.36

A quadratic multiple regression was fitted to the qualified rate, multiple rate and leakage rate to obtain the regression equation

$$\begin{cases} y_1 = 20.07 + 0.8857v_m + 24.62h_g - 0.0496v_m^2 + 0.03178v_m h_g - 2.15h_g^2 \\ y_2 = -1.463 + 0.6943v_m + 0.7894h_g - 0.03086v_m^2 - 0.007v_m h_g - 0.1371h_g^2 \\ y_3 = 81.4 - 1.58v_m - 25.41h_g + 0.8047v_m^2 - 0.02478v_m h_g + 2.287h_g^2 \end{cases} \quad (12)$$

The interaction effects of the working speed and the height of the seed pushers' cams on the qualified rate, multiple rate and leakage rate are shown in Figure 11.

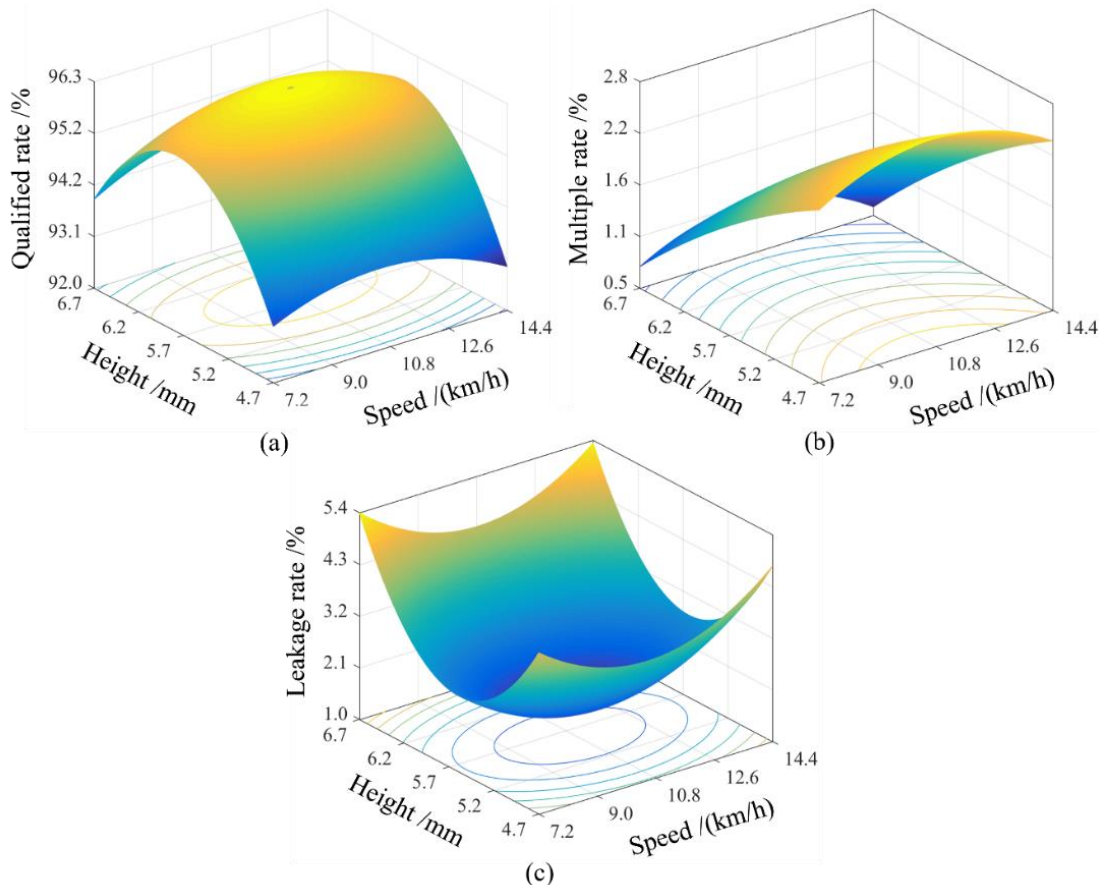


Fig. 11 – Response surface analysis of the interaction effects of factors

Fig. 11(a) shows that when the operating speed is 9.0-12.6 km/h and the height of the convex teeth of the seed pushers is 5.2-6.2 mm, the highest qualified rate is achieved. Fig. 11(b) shows that the lowest multiple rate was achieved when the operating speed was between 9.0 and 12.6 km/h and the height of the convex teeth of the seed pushers was greater than 5.7 mm. Fig. 11(c) shows that when the operating speed is 9.0-12.6 km/h and the height of the convex teeth of the seed pushers is 5.2-6.2 mm, the lowest leakage rate is achieved.

CONCLUSIONS

In this study, in order to improve the uniformity and stability of seed guide delivery, a kind of seed push wheel matched with the drive of the seed discharge tray was designed, the influence of each parameter on the performance of the seed guide was analysed, and the reasonableness of the design was verified by bench test, and it was concluded that the seed guide performance was optimal when the number of the teeth of the seed pusher wheel was 9, the height of the convex teeth of the seed pusher wheel was 5.2-6.2 mm, and the operating speed was 9.0-12.6 km/h.

ACKNOWLEDGEMENT

This work was financially supported by Natural Science Foundation of the Jiangsu Higher Education Institutions of China (23KJB210007).

REFERENCES

- [1] Awad, M., Fouda, O., Abd El-reheem, S., et al. (2022). A new seed drill for planting peas on a raised-bed. *INMATEH - Agricultural Engineering*, 68(3), 681-692. <http://doi.org/10.35633/inmateh-68-67>.
- [2] Chen X., Zhong L. (2012). Design and test on belt-type seed delivery of air-suction metering device. *Transactions of the Chinese Society of Agricultural Engineering*, 28(22), 8-15.
- [3] Du, X., Liu, C. (2023). Design and testing of the filling-plate of inner-filling positive pressure high-speed seed-metering device for maize. *Biosystems Engineering*, 228, 1-17. <http://doi.org/10.1016/j.biosystemseng.2023.02.008>.
- [4] Fanigiliulo, R., Grilli, R., Benigni, S., et al. (2022). Effect of sowing speed and width on spacing uniformity of precision seed drills. *INMATEH - Agricultural Engineering*, 66(1), 9-18. <http://doi.org/10.35633/inmateh-66-01>.
- [5] Im, D., Lee, H., Kim, J., et al. (2023). Bucket size optimization for metering device in garlic planter using discrete element method. *Agriculture (Basel)*, 6(13), 1199. <http://doi.org/10.3390/agriculture13061199>.
- [6] Karayel, D., Güngör, O. & Šarauskis, E. (2022). Estimation of optimum vacuum pressure of air-suction seed-metering device of precision seeders using artificial neural network models. *Agronomy (Basel)*, 7(12), 1600. <http://doi.org/10.3390/agronomy12071600>.
- [7] Kumar-Patel, S., Bhimani, J. B., Yaduvanshi, B. K., et al. (2021). Optimization of the design and operational parameters of planter for vegetable pigeon pea (*cajanus cajan* L. millsp.) seed. *INMATEH - Agricultural Engineering*, 63(1), 326-334. <http://doi.org/10.35633/inmateh-63-33>.
- [8] Li Y., Liu Y., Liu L. (2020). Distribution mechanism of airflow in seed tube of different lengths in pneumatic seeder. *Transactions of the Chinese Society for Agricultural Machinery*, 51(06), 55-64. <http://doi.org/10.6041/j.issn.1000-1298.2020.06.006>.
- [9] Liao Y., Li C., Liao Q., et al. (2020). Research progress of seed guiding technology and device of planter. *Transactions of the Chinese Society for Agricultural Machinery*, 51(12), 1-14. <http://doi.org/10.6041/j.issn.1000-1298.2020.12.001>.
- [10] Liu L., Yang H. (2015). 3D reverse engineering design on seed tube based on Geomagic Design software. *Transactions of the Chinese Society of Agricultural Engineering*, 31(11), 40-45. <http://doi.org/10.11975/j.issn.1002-6819.2015.11.006>.
- [11] Liu Q., He X., Yang L., et al. (2017). Effect of travel speed on seed spacing uniformity of corn seed meter. *International Journal of Agricultural and Biological Engineering*, 10(4), 98-106. <http://doi.org/10.25165/j.ijabe.20171004.2675>.
- [12] Ospanova, S., Aduov, M., Kapov, S., et al. (2024). The results of experimental research of a rotor seed-metering unit for sowing non-free-flowing seeds. *Journal of agricultural engineering (Pisa, Italy)*, 55(1). <http://doi.org/10.4081/jae.2024.1556>.
- [13] Qi B., Zhang D., Liu Q., et al. (2015). Design and experiment of cleaning performance in a centralized pneumatic metering device for maize. *Transactions of the Chinese Society of Agricultural Engineering*, 31(01), 20-27. <http://doi.org/10.3969/j.issn.1002-6819.2015.01.003>.
- [14] Tang H., Wang J., Xu C., et al. (2019). Research progress analysis on key technology of chemical fertilizer reduction and efficiency increase. *Transactions of the Chinese Society for Agricultural Machinery*, 50(04), 1-19. <http://doi.org/10.6041/j.issn.1000-1298.2019.04.001>.
- [15] Yang L., Yan B., Zhang D., et al. (2016). Research progress on precision planting technology of maize. *Transactions of the Chinese Society for Agricultural Machinery*, 47(11), 38-48. <http://doi.org/10.6041/j.issn.1000-1298.2016.11.006>.
- [16] Yuan Y., Bai H., Fang X., et al. (2018). Research progress on maize seeding and its measurement and control technology. *Transactions of the Chinese Society for Agricultural Machinery*, 49(09), 1-18. <http://doi.org/10.6041/j.issn.1000-1298.2018.09.001>.
- [17] Zhao S., Chen J., Wang J., et al. (2018). Design and experiment on v-groove dialing round type guiding-seed device. *Transactions of the Chinese Society for Agricultural Machinery*, 49(6), 146-158. <http://doi.org/10.6041/j.issn.1000-1298.2018.06.017>.